Cerebral Cortex, 2017; 1–12

doi: 10.1093/cercor/bhx046
Original Article

ORIGINAL ARTICLE

Neuronal and Peripheral Pentraxins Modify Glutamate Release and may Interact in Blood–Brain Barrier Failure

Damian M. Cummings[1,*], Tiffanie A. Benway[1,*], Hinze Ho[1,5], Angelo Tedoldi[1,6], Monica M. Fernandes Freitas[1], Lion Shahab[2], Christina E. Murray[3], Angela Richard-Loendt[4], Sebastian Brandner[4], Tammaryn Lashley[3], Dervis A. Salih[1,†] and Frances A. Edwards[1,†]

[1]Department of Neuroscience, Physiology & Pharmacology (NPP), University College London, London WC1E 6BT, UK, [2]Department of Behavioural Science and Health, University College London, London WC1E 6BT, UK, [3]The Queen Square Brain Bank for Neurological Disorders, Department of Molecular Neuroscience, UCL Institute of Neurology, London, UK, [4]Division of Neuropathology and Department of Neurodegenerative Disease, Institute of Neurology, University College London, London WC1N 3BG, UK, [5]Present address: MRC Laboratory of Molecular Biology, Francis Crick Avenue, Cambridge Biomedical Campus, Cambridge CB2 0QH, UK and [6]Present address: Queensland Brain Institute, The University of Queensland, St Lucia, QLD 4072, Australia

Address correspondence to Frances A. Edwards, Department of Neuroscience, Physiology & Pharmacology (NPP), University College London, Gower Street, London WC1E 6BT, UK. Email: f.a.edwards@ucl.ac.uk

[*]Joint first author.
[†]Joint last author.

Abstract

Neuronal pentraxin 1 (NPTX1) has been implicated in Alzheimer's disease, being present in and around dystrophic neurons in plaques, affecting glutamatergic transmission postsynaptically and mediating effects of amyloidβ. Here, we confirm the presence of NPTX1 around plaques in postmortem Alzheimer's disease brain and report that acutely applied human NPTX1 increases paired-pulse ratio at mouse CA3-CA1 hippocampal synapses, indicating a decrease in glutamate release. In contrast, chronic exposure to NPTX1, NPTX2, or NPTX receptor decreases paired-pulse ratio, mimicking some of the earliest changes in mice expressing familial Alzheimer's disease genes. The peripheral pentraxin, serum amyloid P component (SAP), causes similar synaptic effects to NPTX1. The presence of SAP on amyloid plaques in Alzheimer's disease confirms that it can enter the brain. We show that SAP and neuronal pentraxins can interact and that SAP can enter the brain if the blood–brain barrier is compromised, suggesting that peripheral pentraxins could affect central synaptic transmission via this interaction, especially in the event of blood–brain barrier breakdown.

Key words: Alzheimer's disease, central nervous system, neurodegenerative disease, presynaptic, synaptic plasticity

Introduction

Several members of the pentraxin family, the neuronal pentraxins 1 (NPTX1), 2 (NPTX2, also known as neuronal activity regulated pentraxin, NARP), and the neuronal pentraxin receptor (NPTXR) are expressed in neurons of the central nervous system (Schlimgen et al. 1995; Tsui et al. 1996), where, under normal physiological conditions, they modulate synaptic transmission. NPTX1 is constitutively released from excitatory terminals, while release of NPTX2 is activity-dependent (Tsui et al. 1996; Kirkpatrick et al. 2000). In contrast, NPTXR can be membrane-bound, with 1 transmembrane spanning domain, although it has also been shown to have multiple intracellular isoforms (Chen and Bixby 2005). The membrane-bound form can be cleaved enzymatically to release a diffusible form (Kirkpatrick et al. 2000). These 3 pentraxins have effects on postsynaptic glutamate receptors, with NPTX2 alone or in a complex with NPTX1 and NPTXR enhancing α-amino-3-hydroxy-5-methyl-4-isoxazolepropionic acid (AMPA) receptor clustering in excitatory synapses, including those onto parvalbumin-positive interneurons (O'Brien et al. 1999; Xu et al. 2003; Chang et al. 2010; Pelkey et al. 2015). It should be noted that, while the nomenclature NPTX "receptor" comes from the fact that NPTXR was initially hypothesized to be a receptor for the other pentraxins, there is little evidence that the primary mode of action of the other NPTXs is via NPTXR acting as a receptor in the classical sense. The different NPTXs, together or separately, have been implicated in synaptogenesis (Sia et al. 2007; Figueiro-Silva et al. 2015), synaptic plasticity (Xu et al. 2003), synaptic homeostasis (Pribiag and Stellwagen 2014), and metabotropic glutamate receptor-mediated long-term depression (Cho et al. 2008). Moreover, NPTX1 has been implicated in Alzheimer's disease, where it is present in dystrophic neurites around plaques in postmortem brain (Abad et al. 2006), possibly contributing to apoptosis via effects on mitochondria (Clayton et al. 2012). Furthermore, amyloidβ-induced increase in NPTX1 expression has also been implicated in neuronal toxicity (Abad et al. 2006).

In contrast to the NPTXs, the short pentraxin serum amyloid P component (SAP, encoded by the gene *APCS*), is synthesized in the liver (Pepys and Hirschfield 2003). In humans, SAP remains at a fairly stable circulating plasma concentration (~10–100 μg/mL [~0.4–4 μM, based on 25 kDa monomer]; Pepys et al. 1978), while in mice, SAP acts as an acute-phase response protein (Pepys and Hirschfield 2003). Penetration of SAP through the blood–brain barrier is normally poor, resulting in low nanomolar concentrations in cerebrospinal fluid, in both healthy subjects and people with Alzheimer's disease (Kalaria et al. 1991; Hawkins et al. 1994; Kimura et al. 1999). However, this substantial concentration gradient makes SAP a likely candidate for increased penetration to the brain under conditions of blood–brain barrier breakdown, as occurs in many cases of Alzheimer's disease (Blennow et al. 1990; Montagne et al. 2015). Indeed, the presence of SAP on plaques and neurofibrillary tangles in Alzheimer's disease indicates that some penetration indeed occurs (Kalaria et al. 1991). When exogenously applied to central neurons in culture from rat brains, at concentrations found in serum, SAP binds to and enters neurons in vivo and in vitro, resulting in apoptosis (Urbanyi et al. 1994, 2007; Duong et al. 1998). Although these high concentrations are normally unlikely to occur in the brain, with breakdown of the blood–brain barrier the concentration gradient could result in substantial increases in SAP concentrations centrally.

Considering the structural similarity of SAP to the NPTXs, the question arises whether infiltrating SAP could mimic or otherwise interact with these central pentraxins in modulating synaptic transmission in the central nervous system. If SAP is active at central synapses, this could have substantial cognitive consequences, particularly under conditions where a weakened blood–brain barrier results from peripheral inflammation, as commonly occurs in such conditions as urinary tract infections in old age (Manepalli et al. 1990).

The current study focuses on NPTX1, as it has been clearly implicated in Alzheimer's disease and as its expression in glutamatergic synapses in the central nervous system has been shown to be enhanced by amyloidβ (Abad et al. 2006). However, as the 3 NPTXs can function as a complex in synaptic modulation, we have also compared the effects of NPTX2 and NPTXR. Moreover, in light of its penetration into the brain in Alzheimer's disease and likely other conditions of blood–brain barrier breakdown, we confirm that SAP can enter the brain under these conditions and report for the first time that this peripheral pentraxin has potent effects on central excitatory synaptic transmission and interacts with the NPTXs.

Materials and Methods

See Supplementary Materials and Methods for further details.

Purified Native and Recombinant Pentraxin Proteins

Recombinant human NPTXs were obtained from R&D Systems and human native purified SAP from Abcam. Pentraxins were resuspended according to the molecular weight of the monomeric structure and serial dilutions made to obtain working concentrations in culture medium. As the human purified SAP contained sodium azide and ethylenediaminetetraacetic acid, to avoid any off-target effects, the SAP was desalted by buffer exchange as described by Pilling and Gomer (2012).

Animals

Mice transgenic for the human *APCS* (SAP) gene, including 5′ and 3′ flanking sequences (Iwanaga et al. 1989) were backcrossed with C57BL/6J to establish a colony at UCL (TgSAP). Age-matched wild type littermates and C57BL/6J mice were used as controls. C57BL/6J mice were also used for generating organotypic slices. All experiments were performed in agreement with the Animals (Scientific Procedures) Act, 1986 and with local ethical approval.

Organotypic Hippocampal Slices

Organotypic slices were prepared under sterile conditions from 5- to 7-day-old C57BL/6J mouse pups using standard methods (Stoppini et al. 1991; De Simoni et al. 2003; De Simoni and Yu 2006). For slices treated with human pentraxins, SAP or NPTX1, 2 or receptor was dissolved in the culture medium and applied for 7 days starting at 11–17 days in vitro. Both control and treated slices were used for experimentation at 18–24 days in vitro.

Acute Hippocampal Slices

Preparations of acute hippocampal slices were made using standard methods modified from Edwards et al. (1989) adapted for mouse (Cummings et al. 2015). Briefly, mice were killed by decapitation and the brain rapidly removed to ice-cold dissection artificial CSF containing 3 mM Mg^{++} and 0.5 mM Ca^{++}. Slices transverse to the hippocampus were cut and gradually moved to a more physiological (1 mM Mg^{++} and 2 mM Ca^{++})

solution. Slices were allowed to recover at room temperature before experimentation.

Patch-Clamp Recordings

Voltage-clamp (membrane holding potential −70 mV) recordings were made in the whole-cell configuration at room temperature using a CsCl-based internal solution as previously described (Cummings et al. 2015). Pairs of stimuli were applied once every 10 s via a patch electrode filled with artificial CSF, placed extracellularly in the Schaffer-collateral projections.

Field Potential Recordings

Slices were transferred to a heated (30 ± 1°C) submerged chamber, superfused with artificial CSF and allowed to recover for 1 h in the recording chamber. Glass stimulating and recording electrodes (filled with artificial CSF) were positioned in stratum radiatum of CA1 to record a dendritic field excitatory postsynaptic potential (fEPSP). Long-term potentiation conditioning consisted of 5 trains of tetani, each consisting of 100 pulses at 100 Hz, 1.5 s intertrain interval.

Quantitative Real-Time PCR

Quantitative real-time PCR primers were designed to span exon boundaries to distinguish between the PCR amplification from cDNA versus contaminating genomic DNA.

The specificity of the *Apcs* (SAP gene) primers was assessed using cDNA from wild type mouse liver. Forward and reverse primers were incubated with cDNA samples, each primer and KAPA2G PCR ReadyMix, resolved using a 3% agarose gel with ethidium bromide and visualized using Bio-Rad Chemi-Doc MP imaging system. A single band of the predicted product size (155 bp) was observed for the *Apcs* primer pair, with no band observed in the control lanes (cDNA synthesis reaction lacking reverse transcriptase), or in the cDNA from the cortex. To independently assess the specificity of these primers, a melt curve analysis was performed following PCR of liver cDNA on a CFX96 system and by incubating PCR products containing SYBR green PCR mix. A single peak corresponding to one product size was observed for the *Apcs* primers. To assess the efficiency of the primers, a dilution series of the liver cDNA was tested by PCR using the SYBR green PCR mix in triplicate and the data plotted for DNA dilution versus Cq with a line of best fit. The efficiency value for the primer pair was 0.98 with an r^2 value of 0.99, demonstrating the primer pair efficiency was close to 100% with low technical variation.

Generation of Pentraxin Constructs

Total RNA was extracted from hippocampal tissue of mice using the miRNeasy protocol (Qiagen). cDNA synthesis was performed using high-capacity cDNA reverse transcription. The entire cDNA sequence for *Apcs*, *Nptx1*, *Nptx2*, and *Nptxr* was amplified by PCR using the primers listed in Supplementary Table 1 and then subcloned into a plasmid with enhanced green fluorescent protein (GFP)-N1 expression using the EcoRI and BamHI restriction sites upstream of GFP to create a pentraxin-GFP fusion.

Pentraxin Antibodies and Western Immunoblotting

Antibody specificity was tested by Western immunoblotting using lysates from human embryonic kidney (HEK293T) cells overexpressing each of these pentraxin family members individually (Supplementary Fig. 2A,B). The antibodies in Supplementary Table 2 were demonstrated to be specific for the pentraxin they were raised against.

Western blotting was performed using sodium dodecyl sulfate polyacrylamide gel electrophoresis and transfer to nitrocellulose membranes. The membranes were blocked with 5% nonfat milk in Tris-buffered saline with 0.1% Triton-X and then incubated with the appropriate pentraxin antibody (Supplementary Table 2), followed by incubation with horseradish peroxidase-conjugated secondary antibody. Protein bands were visualized using enhanced chemiluminescence.

Coimmunoprecipitation

HEK293T cell lines were transfected with 20 μg plasmid containing GFP-*Nptx1*, -*Nptx2*, -*Nptxr*, -*Apcs* (SAP), empty plasmid, or a combination of two. After a 48 h incubation, cells were washed and scraped into immunoprecipitation (IP) buffer. The coimmunoprecipitation procedure was adapted from that of O'Brien et al. (1999). Briefly, Protein-G and L agarose beads were washed in IP buffer, then coupled to the appropriate antibody (Supplementary Table 2). Following incubation, the beads were washed and the collected cells sonicated then centrifuged. The supernatant was added to the coupled beads and incubated overnight then centrifuged and supernatant collected and frozen. The coupled beads were then washed and protein samples collected by boiling in 3× Laemmli buffer and subsequently diluted to 1× Laemmli for loading.

Immunohistochemistry

Tissue sections (7 μm thick) were cut from the hippocampi of 4 sporadic Alzheimer's disease cases (Table 1). Ethical approval for the study was obtained from the National Hospital for Neurology and Neurosurgery Local Research Ethics Committee. Immunohistochemistry against NPTX1 and SAP (Supplementary Table 2) required antigen retrieval followed by standard immunohistological procedures (Lashley et al. 2011). Color was developed with diaminobenzidine/H_2O_2 and counterstained with hematoxylin.

For mouse brains, immunoperoxidase histochemistry was performed on a Ventana Discovery XT staining platform using the Ventana DAB Map Kit. An in-house monospecific polyclonal rabbit antiserum was used to detect human SAP and a mouse monoclonal antibody was used to detect NPTX1 (Supplementary Table 2). Sections were counterstained with hematoxylin.

Blood–Brain Barrier Breakdown and Entry of SAP into the Brain

In order to test the ability of SAP to cross a compromised blood–brain barrier, a protocol modified from Veszelka et al. (2013) and Bien-Ly et al. (2015) was used. Briefly, 4- to 6-month-old male

Table 1 Postmortem sporadic Alzheimer's disease cases

Case number	Age at onset	Age at death	Duration (years)	Gender
1	80	85	5	M
2	46	52	6	F
3	58	68	10	M
4	54	64	9	M

C57BL/6 mice were given 2 intraperitoneal injections of lipopolysaccharide (LPS, from *Escherichia coli* 0111:B4; Sigma-Aldrich; 100 μg per injection per mouse dissolved in phosphate-buffered saline) or vehicle at 0 and 6 h. Mice then received a further injection of either 250 μg purified native human SAP (Abcam) in 20 mM phosphate buffer or vehicle at 22 h. Mice were perfused with phosphate-buffered saline at 24 h and the brain dissected and snap frozen for Western blot analysis.

Statistics

In order to assess the impact of treatment on paired-pulse ratios, repeated measures ANOVAs were conducted. As experiments were designed such that control experiments were interleaved between the different pentraxin treatments, the control group is common to all experiments. Therefore, to examine the effects of chronic pentraxin treatment, statistical analysis was performed as a one-way ANOVA comparing all treatments. We included the 25 ms interval only, with experiments at longer interpulse intervals performed to ensure the expected depreciating interaction between the 2 excitatory postsynaptic currents (EPSCs) as the paired-pulse interval increases. To examine the effects of acute treatment, a two-way ANOVA was performed, with treatment and time as main effects (time as a repeated measure), as well as a treatment by time interaction term. Where appropriate, post hoc comparisons were conducted, adjusted with the Šidák correction for multiple comparisons. All statistical analyses were performed using Prism6 (GraphPad Software).

All sample sizes are expressed as number of animals. When multiple cells or slices were recorded from one animal, a mean value for that animal was obtained prior to an overall mean ± standard error of the mean (SEM) from all animals. In the case of patch-clamp recordings from organotypic slices, each slice is considered as independent, despite originating from the same pup and, therefore, sample sizes represent the number of slices from which cells were recorded. However, data for each group were obtained from a maximum of 3 slices prepared from any single animal. In all cases, only one cell was obtained from a single slice.

Results

Acute Application of NPTX1 Increases Paired-Pulse Ratios at Schaffer-Collateral Synapses

Initially, to investigate whether we could detect acute effects of NPTX1 on synaptic transmission in the hippocampus, patch-clamp recordings of EPSCs from CA1 pyramidal neurons were conducted in organotypic hippocampal slices. EPSCs were recorded in response to pairs of electrical stimuli applied every 10 s to Schaffer collaterals in the presence of the $GABA_A$ (γ-aminobutyric acid) receptor antagonist, gabazine (6 μM). Paired-pulse ratios (the amplitude of the second divided by amplitude of the first of a pair of response) were determined in order to test for alterations in probability of glutamate release, with the probability of release of transmitter in response to the first stimulus inversely proportional to paired-pulse ratio (Zucker 1989; Dobrunz and Stevens 1997). As expected at this synapse, paired-pulse facilitation was observed across all control experiments (Fig. 1). The interpulse interval between each pair of stimuli was set at 25 ms. After a 5-min period of stable baseline recording, NPTX1 (60 nM) was added to the perfusion medium and stimulation continued. There was no change in paired-pulse ratio over time when no pentraxin was included in the bath solution. In contrast, when NPTX1 was washed onto the slice, the paired-pulse ratio increased (Fig. 1A), suggesting that acute application of NPTX1 decreases the release probability of glutamate. As control experiments were interleaved with those for NPTX1 and SAP (see below), control data are common to both. A significant interaction of treatment and time ($P < 0.05$) was observed and Šidák post hoc multiple comparisons showed significance at both the 5- and 10-min time points.

Chronic Application of Neuronal Pentraxins Decreases Paired-Pulse Ratio and Down Regulates Response to Acute Application

Considering the direct effect of NPTX1 on glutamate release when applied acutely and the evidence that expression of NPTX1 is increased in the presence of amyloidβ, we went on to examine the effect of constant exposure of organotypic slices to low levels of NPTX1 over 7 days. In contrast to acute application, chronic application of NPTX1 resulted in a dose-dependent decrease in paired-pulse ratios, with significant effects at 60 and 100 nM (Fig. 1B; summarized in Fig. 1F). Note that, in these chronic experiments, NPTX1 was applied to the culture medium of the organotypic slices over 7 days but little, if any, would be present in the perfusion solution during recording after a minimum of 30 min washing. Hence, once the NPTX1 is washed out after chronic exposure, the probability of glutamate release in control solution goes in the opposite direction from the effect of acute exposure. This presumably reflects a homeostatic response, maintaining the network balance during the long-term presence of this synaptic modulator.

In a subsequent series of experiments, to test the effect of acute application after chronic exposure, we applied acute NPTX1 (60 nM) to slices that had been chronically treated as above. Under these conditions, the effect of acute application was completely lost (Fig. 1A) demonstrating a down-regulation of the response to acute NPTX1 after chronic exposure. Hence, assuming that there is physiologically some ongoing release of NPTX1, the paired-pulse ratio in control solution would be slightly increased compared with the paired-pulse ratio in the complete absence of NPTX1 (or similarly acting neuromodulators). However, after chronic exposure, the loss of the effect of acute NPTX1 would prevent the endogenous modulation. This would be compatible with the decrease in paired-pulse ratio (increased release probability) resulting from chronic exposure.

Chronic application of NPTX2 or NPTXR (Fig. 1C,D, respectively; summarized in Fig. 1F) was found to have similar effects to NPTX1, with NPTXR having a potency in the same range as NPTX1. NPTX2 was rather less potent, with no measureable effects at 70 nM but increasing release probability at the highest concentration of 420 nM.

As the chronic experiment was designed such that control experiments were interleaved between the different pentraxin treatments, the control group is common to all experiments. Therefore, statistical analysis was performed as a single one-way ANOVA, considering the 25 ms interval only ($P < 0.0001$). The 25 ms interval paired-pulse ratios are summarized in Figure 1F, where Šidák post hoc multiple comparisons are shown, comparing each pentraxin treatment to control. Note that the acute application of NPTX1, after chronic exposure, was a subsequent series of experiments and hence had controls interleaved with treated slices independently of the above.

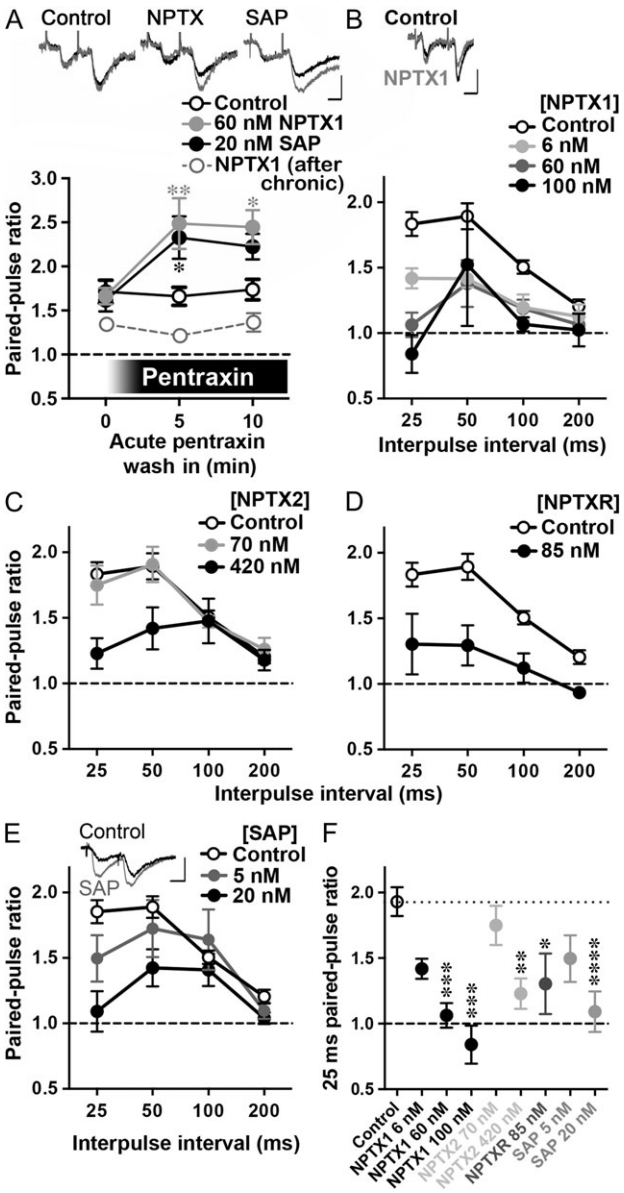

Figure 1. Pentraxins modulate probability of glutamate release at CA3-CA1 synapses. Voltage-clamp recordings from CA1 pyramidal neurons in response to pairs of stimuli to Schaffer collaterals in hippocampal organotypic slices. (*A*) Acute application of NPTX1 ($n = 9$ slices) or SAP ($n = 8$) increased paired-pulse ratio at 25 ms interpulse interval. In each slice, 15 traces were averaged across 5 min preceding the indicated time point. *$P < 0.05$; **$P < 0.01$. Šidák post hoc multiple comparisons compared with time-matched control ($n = 6$). In a different series of experiments, effects of acute application of 60 nM NPTX1 on paired-pulse ratio are shown in slices pretreated for 7 days with 60 nM NPTX1 ($n = 8$). Traces show typical paired-pulse ratio responses at 25 ms interpulse intervals from control and pentraxin-treated slices. Black traces: baseline (0 min); gray traces: 5 min treatment. Scale bar: 10 pA x 10 ms. (*B*) Treatment with recombinant human NPTX1 for 7 days resulted in a dose-dependent decrease in paired-pulse ratio. Control $n = 26$; 6 nM, $n = 6$; 60 nM, $n = 7$; 100 nM, $n = 4$ slices. Traces show typical paired-pulse ratio responses at 25 ms interpulse intervals from control (black) and NPTX-treated (gray) slices. Scale bar: 10 pA x 5 ms. (*C*) Treatment with recombinant human NPTX2 for 7 days gave rise to a dose-dependent decrease in paired-pulse ratio. Control $n = 26$; 70 nM, $n = 4$; 420 nM, $n = 7$ slices. (*D*) Treatment for 7 days with recombinant human NPTX receptor ($n = 5$) also decreased paired-pulse ratio compared with control ($n = 26$). (*E*) Treatment with human SAP for 7 days reduced paired-pulse ratios in a dose-dependent manner. Control $n = 26$ (same control preparations in *B*, *C*, and *D*); 5 nM, $n = 5$; 20 nM, $n = 9$ slices. Traces show typical responses from paired-pulse stimuli at 25 ms interval from control (black) and SAP-treated (gray) slices. Scale bar: 10 pA x 10 ms. (*F*) Summary data of the chronic application of pentraxins, showing only paired-pulse ratios from 25 ms interpulse intervals. One-way ANOVA was highly significant ($P < 0.0001$). Šidák post hoc multiple comparisons are shown compared with control, *$P < 0.05$; **$P < 0.01$; ***$P < 0.001$; ****$P < 0.0001$. Panels A–F are presented as mean ± SEM across slices.

Exposure of Hippocampal Synapses to the Peripheral Pentraxin SAP has Similar Effects to Neuronal Pentraxins

As expected, we detected no significant expression of SAP at the RNA level in the hippocampus, cortex or cerebellum of 4 months old wild type mice using PCR (Supplementary Fig. 1A). Similarly, no expression of SAP was detected using microarray analysis of these brain regions of wild type mice or mice transgenic for genes for familial Alzheimer's disease at 2, 4, 8, and 18 months of age (www.mouseac.org; see Matarin et al. 2015). This is as expected, as SAP is an acute-phase protein in mice (Baltz et al. 1980; Bottomley et al. 1988) most likely expressed exclusively in the liver (Yasojima et al. 2000; Mulder et al. 2010; Hawrylycz et al. 2012; www.brain-map.org). However, SAP has been reported to be detectable in the cerebrospinal fluid (Hawkins 1994) and on plaques (Kalaria et al. 1991) of Alzheimer's disease patients and so, to reach the concentrations reported in CSF, must penetrate the blood–brain barrier, possibly due to blood–brain barrier breakdown. We thus investigated whether SAP has direct effects upon synaptic transmission in the central nervous system. Native purified human SAP (20 nM) applied acutely to organotypic slices also had a similar effect to the acute application of NPTX1, resulting in an increase in paired-pulse ratio (Fig. 1A), suggesting that SAP can also have direct effects by decreasing glutamate release probability.

SAP was also added chronically to the culture medium of hippocampal organotypic slices exactly as for the NPTXs above. Hence, the effect of applications of SAP (0, 5, and 20 nM) were compared with the effects of similar concentrations of NPTX1 after 7-day exposure and, like NPTX1, paired-pulse ratios were decreased in a dose-dependent manner, again suggesting an increase in release probability (Fig. 1E; summarized in Fig. 1F). Together these results suggest that SAP and NPTX1 have similar, potent presynaptic effects at CA3-CA1 synapses.

Effects of Transgenic Expression of Human SAP in Mice In Vivo

As SAP is expressed in the liver, we tested whether the effects seen above would occur if human SAP was expressed on the human SAP promoter in the liver of transgenic mice (Iwanaga et al. 1989). These mice have a steady state SAP plasma concentrations within the human range (ibid). Acute hippocampal brain slices were prepared from 14-month-old animals and patch-clamp experiments were performed. Interestingly, these mice showed an even greater decrease in paired-pulse ratio than seen with the 7-day application of SAP, with almost no facilitation seen throughout the interpulse intervals used and thus significant differences between the SAP and WT mice at all interpulse intervals between 25 and 100 ms (Fig. 2A). A statistically significant genotype by interval interaction ($P < 0.01$) was also observed, reflecting the lack of the usual effect of increasing the interval between pulses in the transgenic mice.

In acute slices, it is possible to use minimal stimulation in which only one or a few axons is stimulated, thus allowing the analysis of failures to release transmitter. In order to verify that the changes in paired-pulse ratio represented a change in

release probability in the SAP transgenic mice the effect of minimal stimulation was tested to isolate one or very few CA3 axons. The mean failure rate was lower in SAP mice than in wild type littermates (Fig. 2*B*), confirming an increase in glutamate release probability, consistent with the decreased paired-pulse ratios.

In the same cohort of animals, we recorded field potentials from CA1 stratum radiatum in response to stimuli applied to Schaffer collaterals in acute brain slices. Responses tended to be larger in transgenic SAP mice (Fig. 2*C*) and, similarly to the voltage-clamp recordings above, paired-pulse ratios were lower (Fig. 2*D*). The magnitude of long-term potentiation induced by a tetanic stimulus was significantly smaller in slices from SAP mice compared with wild type mice (Fig. 2*E*). So again, it is clear that central transmission and, furthermore, synaptic plasticity can be influenced in mice with SAP levels tonically raised lifelong, due to expression of human SAP from the liver.

When considered together, the data from exogenous application of SAP to organotypic brain slices and experiments performed in acute brain slices from transgenic animals expressing human SAP, clearly demonstrate that chronic exposure to SAP positively modulates glutamate release and that sufficient SAP can enter the brain of the mouse to cause this effect, even when only expressed in the liver. Moreover, with long-term exposure, the magnitude of long-term potentiation was also reduced.

NPTX1 and SAP Interact When Applied to Organotypic Slices or When Overexpressed in Human Embryonic Kidney Cells

NPTX1 (6 nM; submaximal concentration) was included in the culture medium of organotypic slices for 7 days (as above) together with SAP (5 or 20 nM) and the effects compared with interleaved experiments comparing NPTX1 or SAP alone at the same concentrations. As the interleaved experiments were not different from the previous experiments using these concentrations, the data were pooled (Fig. 3*A*,*B*). SAP affected paired-pulse ratio alone at both concentrations as did 6 nM NPTX1 but combining NPTX1 and SAP did not result in an additional effect to that of application of NPTX1 alone. As described above, pentraxin treatments and experiments, where no pentraxin was applied, were interleaved and thus controls are common to all experiments and thus statistical analysis performed as a single one-way ANOVA ($P < 0.0001$). The absence of an additive effect of coapplication suggests that the 2 pentraxins are not acting independently but interact with the same target when applied together. Moreover, this implies that, when SAP enters the brain, it could interact with the endogenously released NPTX1, either at the level of NPTX1 or at downstream targets.

To investigate the possible interactions of central and peripheral pentraxins further, HEK cells were cotransfected with pairs of NPTXs, or with SAP and a NPTX. The possibility of complex

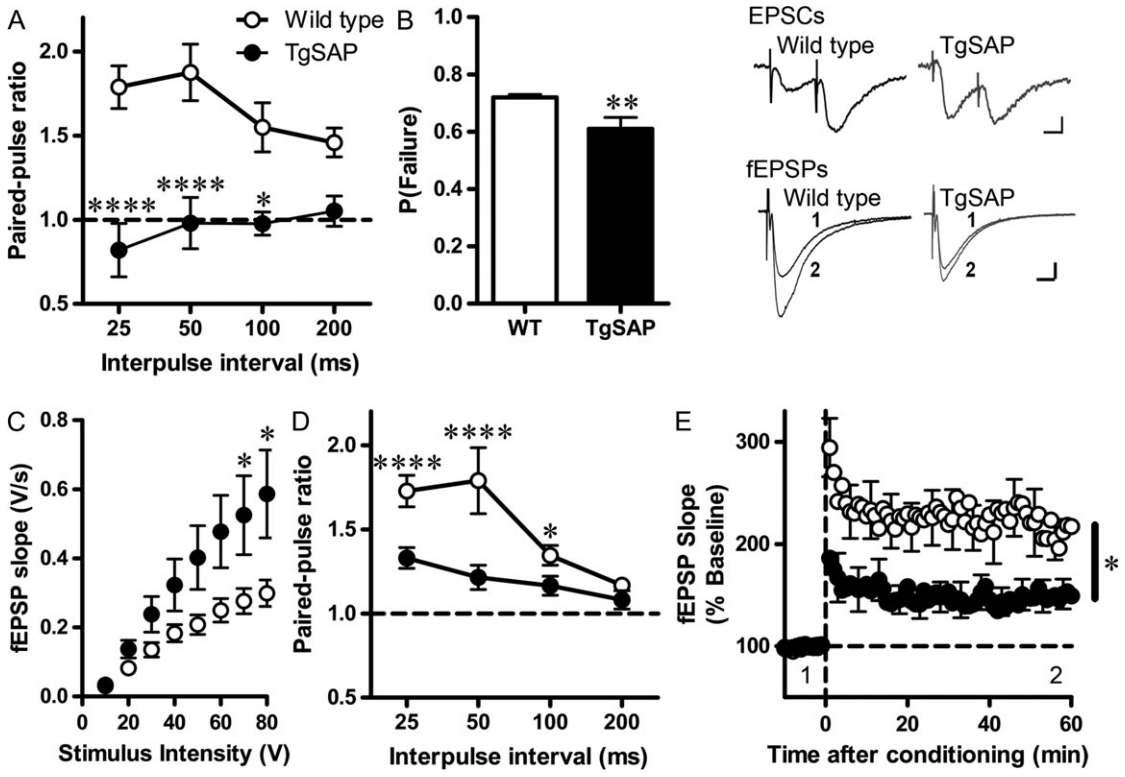

Figure 2. Transgenic expression of human SAP reduces paired-pulse ratio and long-term potentiation at CA3-CA1 synapses. Acute hippocampal brain slices were prepared from TgSAP mice expressing human SAP on its own promoter and field potentials recorded from stratum radiatum in response to Schaffer-collateral stimulation. (*A*) Paired-pulse ratios measured with voltage-clamp were lower in slices from transgenic animals ($n = 9$ animals) compared with controls ($n = 8$). Repeated measures ANOVA revealed an interaction between genotype and interval ($P < 0.02$). Šidák post hoc comparison to control at the same interpulse interval are indicated *$P < 0.05$; ****$P < 0.0001$. The example EPSCs (top right panel) are from the 25 ms interpulse interval. Scale bar: 5 pA x 10 ms. (*B*) Failure rate for evoked EPSCs at minimal stimulation (WT, $n = 7$; TgSAP, $n = 5$ animals; **$P < 0.01$, unpaired *t*-test). (*C*) Input–output relationships for fEPSPs at CA3-CA1 synapses in slices from WT ($n = 9$ animals) and TgSAP ($n = 8$ animals). (*D*) Paired-pulse ratios determined from fEPSPs evoked in slices from WT and TgSAP mice. (*E*) Long-term potentiation was induced by tetanic stimulation at time zero (vertical dashed line). Two-tailed unpaired *t*-test comparing the means of the last 10 min is indicated by *$P < 0.05$. Example fEPSPs are shown above from the approximate times indicated by 1 and 2. Scale bar: 0.2 mV × 5 ms. Panels *A*–*E* are presented as mean ± SEM.

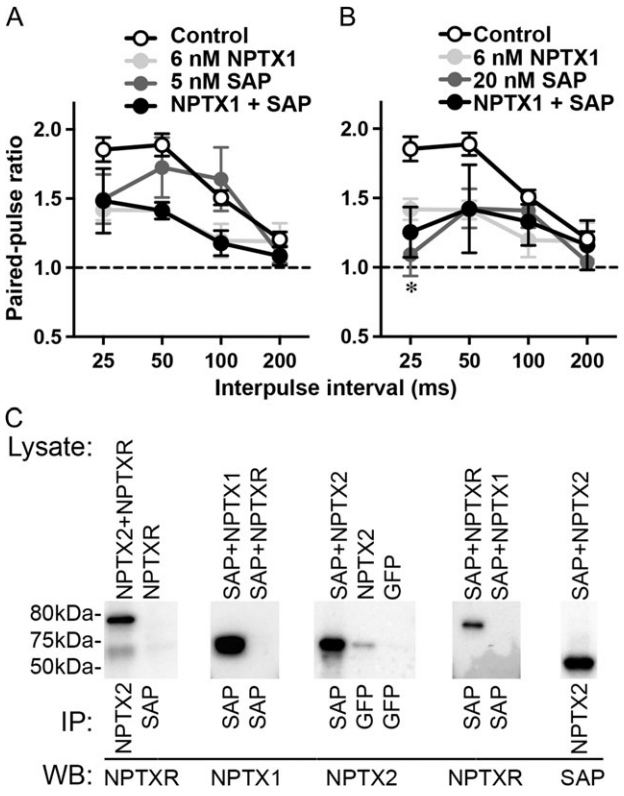

Figure 3. SAP forms complexes with each of the NPTXs and affects synaptic transmission. (*A*,*B*) Effect of coapplication of NPTX1 and SAP on paired-pulse ratios at CA3-CA1 synapses. (*A*) Comparison of 6 nM NPTX1 and 5 nM SAP applied individually or together. Control, $n = 26$; 6 nM NPTX1, $n = 6$; 5 nM SAP, $n = 5$; NPTX1 and SAP, $n = 6$ slices. (*B*) Comparison of 6 nM NPTX1 and 20 nM SAP applied individually or together. Control, $n = 26$; 6 nM NPTX1, $n = 6$; 20 nM SAP, $n = 9$; NPTX1 and SAP, $n = 6$ slices. Šidák post hoc comparisons are shown for coapplication versus control at 25 ms intervals $^*P < 0.05$. Panels *A* and *B* are presented as mean ± SEM. (*C*) HEK293T cells were transfected with constructs expressing the combinations of pentraxins indicated, each fused to GFP. After 48 h, lysates were collected and tested by IP followed by Western blotting (WB) with antibodies specific to each pentraxin. The bands correspond to the molecular weight predicted for each full-length pentraxin fused to GFP, with molecular weights for GFP ~27 kDa, SAP ~25 kDa, NPTX1/2 ~47 kDa, and NPTXR ~53 kDa (Supplementary Fig. 2A,B). Note: the NPTX1 and NPTXR antibodies were not effective at IP, even for NPTX1 and NPXTR themselves, in part due to lower affinity (see Supplementary Fig. 2D).

formation was subsequently tested by coimmunoprecipitation. Considering the similarity in structure of the NPTXs and SAP, we tested the specificity of the antibodies by overexpressing each individual pentraxin in HEK cells and subsequent Western immunoblot and identified a specific antibody for each pentraxin (Supplementary Fig. 2A,B). The relative affinity of each of these specific pentraxin antibodies to its respective target was determined using serial dilutions of purified/recombinant pentraxin proteins, with concentrations of all the purified/recombinant pentraxins independently verified (Supplementary Fig. 2C,D). The SAP antibody showed higher affinity than the NPTX1 antibody (Supplementary Fig. 2D). As reported previously, NPTX1, NPTX2, and NPTXR can form heteropentamers (Kirkpatrick et al. 2000; Xu et al. 2003) as reflected here in their coimmunoprecipitation when expressed together in HEK cells (Fig. 3C). Interestingly, SAP was also found to form a complex with NPTX1, NPTX2, or NPTXR (Fig. 3C), thus further suggesting that the effects of SAP on synaptic transmission could be due to interactions with the NPTXs.

SAP and NPTX1 Accumulate Around Plaques in Hippocampus and Cortex of Alzheimer's Patients

Considering, in different reports, both NPTX1 and SAP have been reported to be associated with neuritic plaques in postmortem brain tissue of people with Alzheimer's disease, we went on to compare the localization of these pentraxins in postmortem brains from Alzheimer's patients using the antibodies, the specificity of which we had established above (Supplementary Fig. 2A,B). NPTX1 showed very strong staining of dystrophic neurites around the periphery of plaques as well as a general diffuse staining between the neurons but little, if any, staining in the core of the plaque. In addition, there was a general punctate staining of nerve terminals throughout the tissue. This staining of nerve terminals reflects the normal distribution of NPTX1 as seen in human (Fig. 4A) or wild type mouse brains (Fig. 4B). In the Alzheimer's disease human postmortem brain, NPTX1 staining was also seen in dystrophic neurons remote from plaques, which may represent neurons with tau pathology (Fig. 4Aii).

SAP staining was also seen in association with plaques in postmortem brains from Alzheimer's disease patients (Fig. 4C). Although very faint, this staining was present diffusely around the plaques but was not evident elsewhere in the tissue. As the SAP antibody showed higher affinity than the NPTX1 antibody for their respective targets (Supplementary Fig. 2D), the relative strength of antibody staining suggests that only relatively little SAP is present on the plaque compared with NPTX1. This is perhaps not surprising as the NPTX1 is produced in glutamatergic nerve terminals and so this staining likely represents locally released NPTX1, possibly from the dystrophic neurites themselves. Hence, unless structural changes of the proteins when bound around amyloid plaques results in a differential change in the binding of the antibodies, the pentraxin binding to plaques is strongly dominated by the NPTX, NPTX1, when compared with SAP. Little, if any, specific staining was detected in the hippocampus of SAP transgenic mice, although some staining was evident in the fimbria (Fig. 4D).

SAP Can Enter the Brain When the Blood–Brain Barrier is Compromised

Under normal conditions, SAP would not be expected to cross the blood–brain barrier and yet we know that it can enter the brain in Alzheimer's disease as evidenced by its presence on plaques. We hypothesize that it could cross under conditions of blood–brain barrier breakdown as has been reported to occur in AD or under conditions of inflammation or other disease conditions. While soluble SAP would be expected to be broken down or be otherwise removed from the brain (Veszelka et al. 2013), its binding to plaques could prevent its removal. We thus tested for levels of mouse and/or human SAP in the brain using Western blot in wild type mice after injection of human SAP with or without compromising the blood–brain barrier by treatment with LPS (Fig. 5; Veszelka et al. 2013; Chisholm et al. 2015). In the absence of LPS, we could detect only very low levels of SAP in the brain of untreated mice or mice injected with human SAP (250 μg). However, 22 h after the first of 2 LPS administrations, injection of human SAP resulted in a strong signal in both hippocampus and cerebellum. Furthermore, even without injection of human SAP, endogenous mouse SAP levels were increased in the brain, albeit at rather variable levels (Fig. 5). Two-way ANOVA confirmed a significant effect of LPS ($P = 0.01$) and no significant effect of SAP injection and no interaction.

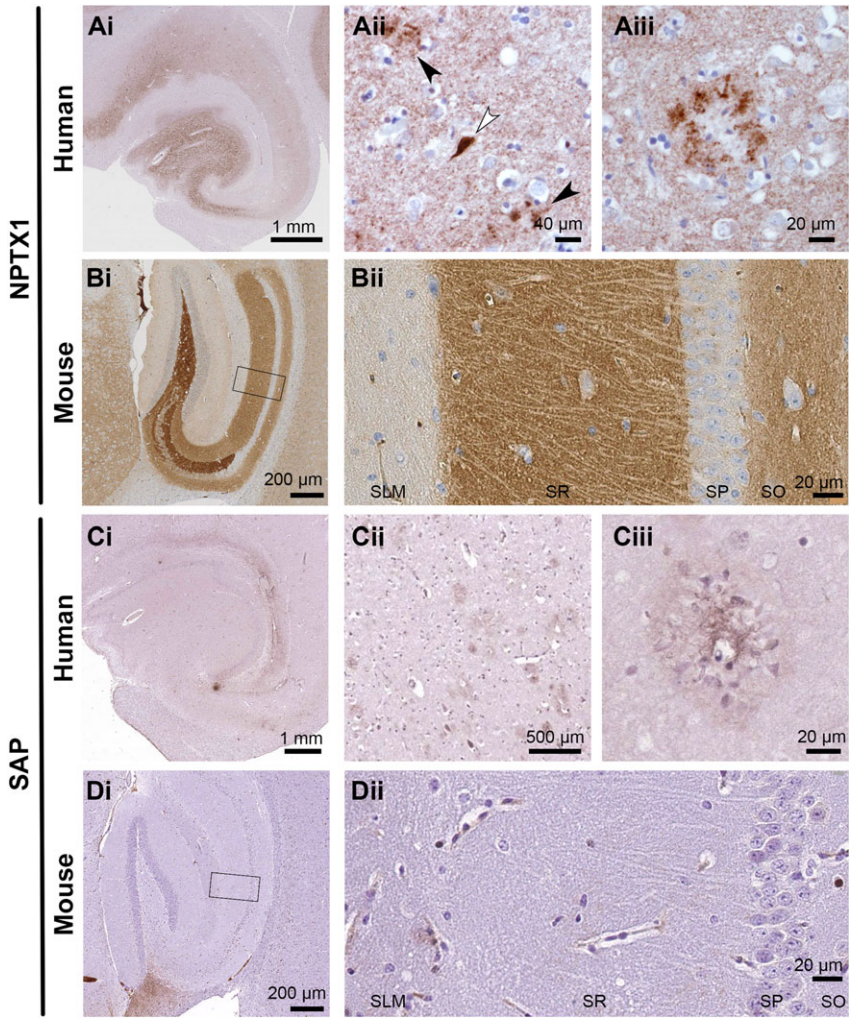

Figure 4. Comparison of the distribution of NPTX1 and SAP in glutamatergic terminals and on amyloid plaques. (*A*) Postmortem Alzheimer's hippocampus stained for NPTX1 (brown diaminobenzidine staining). (*Ai*) NPTX1 is evident in the hippocampus, particularly within the polymorphic layer of the dentate gyrus, stratum lucidum of CA3 and stratum radiatum of CA1. 4× objective. (*Aii*) A neurofibrillary tangle (white arrowhead) distal to neuritic plaques (black arrowheads) in the hippocampus. Both are heavily stained for NPTX1. 20× objective. (*Aiii*) A higher magnification (40× objective) image showing NPTX1 associated with a neuritic plaque in the temporal cortex. (*B*) NPTX1 staining in the hippocampus of an adult wild type mouse. Note the similar pattern of staining to human (i.e., polymorphic layer of dentate gyrus, particularly heavy staining in stratum lucidum of CA3 and lighter staining in stratum radiatum of CA1; but in the case of the mouse, also in all layers of CA3 and in stratum oriens in CA1). (*Bii*) Higher magnification image of the CA1. The area of interest is indicated in (*Bi*). Note the presence of NPTX1, particularly in stratum radiatum (SR) and stratum oriens (SO) but a near-absence in stratum pyramidale (SP) and stratum lacunosum moleculare (SLM). (*C*) Postmortem AD hippocampus stained for SAP. (*Ci*) Note the lower level of staining compared with NPTX1. 4× objective. (*Cii*) Cortical plaques stained for SAP. (*Ciii*) Higher magnification image (40× objective) of plaques stained for SAP. (*D*) Transgenic SAP mouse hippocampus stained for SAP. (*Di*) Little (if any) specific staining. (*Dii*) Higher magnification image of CA1. Area of interest indicated by box on *Di*. Panels *A*–*D*: brown staining is NPTX1 or SAP.

Discussion

Novel Effects of Pentraxins on Synaptic Transmission

NPTX1 and NPTX2 have previously been shown to affect postsynaptic elements of glutamatergic synapses in the hippocampus causing clustering of AMPA receptors (Xu et al. 2003). We confirm here the distribution of NPTX1 in hippocampal glutamatergic nerve terminals, as reported by Cho et al. (2008). Moreover, we demonstrate here for the first time that all 3 NPTXs and also the peripheral pentraxin SAP have effects presynaptically, strongly decreasing paired-pulse ratio when added to the culture medium of organotypic slices over a 7-day period. This also occurs in transgenic mice overexpressing human SAP. Moreover, in the latter case, experiments using minimal stimulation confirmed that failure rates decreased and thus that the change in paired-pulse ratio was due to an increase in glutamate release probability.

Interestingly, when NPTX1 or SAP was added acutely, the opposite effect was seen with an increase of paired-pulse ratio, suggesting that the direct effect of the pentraxins is a decrease in probability of evoked glutamate release. The observation that acute effect of NPTX1 is lost, after chronic exposure, suggests that the effect of chronic application is a homeostatic reaction, decreasing the sensitivity to acute pentraxins. Hence, when the background pentraxin level is chronically raised by adding NPTX1 to the culture medium, rather than the release of glutamate remaining low, physiologically released pentraxins lose their efficacy so that compared with untreated synapses the average release probability is increased. It is possible

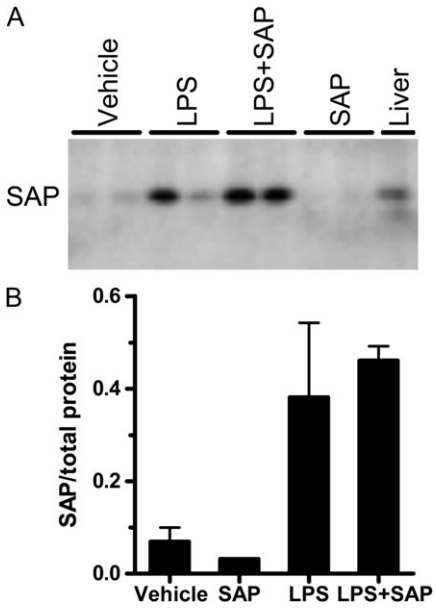

Figure 5. SAP crosses the compromised blood–brain barrier. Mice were administered LPS to compromise the blood–brain barrier, injected with native human SAP and hippocampus probed for SAP. (*A*) Western blot showing SAP levels in the 4 groups of mice. Liver from an animal injected with SAP is shown in the last lane as a positive control. (*B*) SAP levels were normalized to total protein levels (Ponceau-S). Data presented as mean ± SEM from 2 animals per group. Main effect of LPS, $P = 0.01$ (two-way ANOVA).

that the clustering of AMPA receptors, previously reported, is a homeostatic response to overexpression of the NPTXs, as this would also increase the efficacy of glutamate transmission (Xu et al. 2003). Moreover, it has been suggested that pentraxins could have an intracellular mode of action, as evidenced by the apoptosis-induced upregulation of NPTX1, which targets mitochondria, leading to their fragmentation (Clayton et al. 2012). Indeed, mitochondrial regulation of calcium within the presynaptic terminal can modulate glutamate release (Scotti et al. 1999).

The question arises as to how the acute and chronic application of the pentraxins in organotypic slices relate to the effects of pentraxins in vivo. Figueiro-Silva et al. (2015) examined the effects of NPTX1 in vivo using lentivirus knockdown of NPTX1. Interestingly, they observed enhanced long-term potentiation but no change in paired-pulse ratio of field EPSPs recorded in behaving mice. Unless prevented by compensation (e.g., by upregulation of other NPTXs), the knockdown of NPTX1 would be expected to have the same effect as chronically applied NPTX1 used in the present study in which the effect is lost due to desensitization rather than lack of the protein. Considering the similarity in the effects of the different pentraxins observed in the present study, the lack of effect on paired-pulse ratio after knockdown, likely suggests that other pentraxins are upregulated to compensate or that the sensitivity to the remaining NPTX1 is increased under these conditions. In contrast, after high-frequency stimulation, the differences in synaptic plasticity were seen in the above study, with the enhancement of responses evident over several days. In acute hippocampal slices from the SAP transgenic mouse (that mimic the effects of chronic exposure to NPTXs), long-term potentiation was impaired. This is consistent with the enhancement reported by Figuero-Silva et al. in the mouse after knockdown of NPTX1.

How Does This Relate to Alzheimer's Disease?

Both SAP and NPTX1 have been reported previously and are confirmed here, to be present on amyloid plaques in Alzheimer's disease. In the present study by comparing the 2 pentraxins under similar conditions, we can compare the relative amounts of SAP to NPTX1 on plaques. The question arises as to whether they play an active role in the disease in this or other contexts. The present study suggests that, while they are both present on plaques, NPTX1 dominates and so the effect of SAP would be, at most, subtle. Although it is not impossible that low levels of SAP may influence the deposition of amyloidβ, what is clear that its presence on plaques in postmortem brains is indicative of its ability to enter the brain. This suggests that the effects observed here of soluble SAP on synaptic transmission, at very low concentrations, could be important physiologically, resulting in profound effects on neuronal function, particularly when increased by blood–brain barrier breakdown, as reported in Alzheimer's disease (Blennow et al. 1990; Montagne et al. 2015). We suggest that the synaptic effects of SAP probably involve the same pathways as the effects of NPTXs and are possibly due to direct molecular interaction between the pentraxins.

A further observation of interest in these experiments in human brain was that all the dystrophic neurites within the plaque showed strong NPTX1 staining. As there is no evidence of NPTX1 being taken up by dendrites, this would suggest that the neurites seen in plaques are axonal boutons, rather than dendrites.

Recently, we have reported in mice transgenic for genes that cause familial Alzheimer's disease (hemizygous TASTPM; $APP_{Swe}/PSEN1_{M146V}$) that the first effect of rising amyloidβ is an increase in glutamate release probability (Cummings et al. 2015), very similar to that reported here after chronic exposure to NPTXs. This is consistent with the effect of amyloidβ in normal rats when released in response to specific stimulus paradigms (Abramov et al. 2009) and would be compatible with reports that some of the effects of amyloidβ may be mediated by increasing NPTX1 expression (Abad et al. 2006).

Is Infiltration of SAP into the Brain Likely to Affect Synaptic Transmission Under Other Conditions?

The present study clearly shows that SAP can have effects on synaptic transmission when applied to organotypic slices at low nanomolar concentrations. Moreover, the concentration gradient between plasma and brain is reported to be in the region of 1000-fold (Nelson et al. 1991; Kolstoe et al. 2009) and thus, in cases of blood–brain barrier breakdown, SAP concentrations could increase markedly, directly affecting synaptic transmission or, perhaps more likely, interacting with released NPTXs. The observation that SAP can enter the brain under conditions of blood–brain barrier breakdown is thus compatible with the reported 1000-fold concentration gradient between plasma and brain (Nelson et al. 1991; Kolstoe et al. 2009).

Infiltration of SAP into the brain under conditions of blood–brain barrier breakdown would be relevant not only to Alzheimer's and other diseases in which prolonged blood–brain barrier breakdown occurs (Blennow et al. 1990), but also to conditions such as stroke and other vascular incidents or during various types of inflammation. Under such conditions, spikes of SAP infiltrating the brain could have major short-term effects on cognition. It is interesting that similar effects are seen in mice with human SAP expressed in the liver, suggesting that sufficient SAP can enter the brain to have effects, even under

physiological conditions. Interestingly, the synaptic effects of SAP in the transgenic mice also resulted in a decrease in long-term potentiation in response to tetanic stimulation. It seems likely that the greatly increased release probability observed in the transgenic mice is directly related to the loss of long-term potentiation. This could result in a rapid depletion of readily available vesicles during high-frequency stimulation leading to failure of synaptic transmission during the conditioning train, hence decreasing the time course of Ca^{2+} influx on which the plasticity depends.

The question arises as to how the SAP gets into the brain of the transgenic mice. It is possible that SAP is having an effect peripherally that results in changes in factors that can cross the blood–brain barrier, rather than SAP itself entering the brain. However, the similarity between the effects of exogenously applied SAP and the insertion of a transgene for SAP into mice suggests that the effects seen are directly due to the presence of SAP in the brains of the transgenic animals. We find that exogenously applied SAP has effects at concentrations as low as 20 nM, if the organotypic slice is exposed for 7 days. The transgenic mice are exposed to SAP throughout life and so it is possible that even lower levels can modulate synaptic transmission under these conditions. On the other hand, it is also possible that the blood–brain barrier is compromised from time to time during the life of the mouse and that this results in slightly higher levels in the brain. Finally, although we and others (Mulder et al. 2010; Hawrylycz et al. 2012 [www.brain-map.org]; Matarin et al. 2015 [www.mouseac.org]) find little or no evidence for expression of SAP within the brain, there still remains the possibility of local synthesis (Yasojima et al. 2000) which may be below detection thresholds in most studies. Whatever the final concentrations within the synapse, it is clear that very low levels of SAP in the brain can result in changes to synaptic transmission.

How is SAP Affecting Synaptic Transmission?

The most likely explanation for the effects of SAP on central synaptic transmission is that it is mimicking the structurally related NPTXs, which are highly expressed in the brain. The fact that its effect when coapplied with NPTX1 is not additive suggests that, at some level, they are interacting or affecting the same targets. The observation that SAP and the NPTXs can be pulled down together in coimmunoprecipitation experiments suggests that SAP may be able to contribute to heteromultimeric complexes of NPTXs, altering their activity. However, it is also possible that they are pulled down together because they can simultaneously bind to other common partners.

Moreover, although SAP and NPTX1 are both present around amyloid plaques in postmortem brains of people with Alzheimer's disease, only NPTX1 appears elsewhere in the hippocampus and cortex. Hence, while NPTX1 is clearly present in presynaptic terminals in both mouse and man, we see no evidence of the presence of intracellular SAP in hippocampus or cortex even when expressed transgenically on a WT mouse background. Thus, the effect of SAP on synaptic transmission in the transgenic mice is presumably due to the presence of soluble SAP in the extracellular space, which is washed out when the brain is perfused during tissue preparation, rather than due to formation of pentamers within the neurons. It is thus more likely that the interaction relates to competition between these closely related molecules rather than direct interaction between the peripheral and central pentraxins, although this can also occur.

In conclusion, the NPTXs have strong presynaptic effects on glutamatergic transmission in the CNS at low nanomolar concentrations and particularly NPTX1 is widely distributed throughout the synaptic terminals of the hippocampus and cortex. It is interesting to note that all the pentraxins tested have similar effects on synaptic transmission, although NPTX2 shows a rather lower potency. Considering previous reports of postsynaptic effects of NPTX2 and other NPTXs (O'Brien et al. 1999; Xu et al. 2003; Chang et al. 2010), this may suggest that the primary effects of different NPTXs may differ, resulting in complementary, if overlapping, effects on synaptic transmission.

We confirm previous reports that sufficient concentrations of the peripheral pentraxin, SAP, enter the brain in Alzheimer's disease for it to be detectable on plaques, albeit modestly compared with NPTX1. Independent of interactions with plaques, the interaction of SAP with the NPTXs may also cause disruption to the normal synaptic effects of NPTXs in the brain. Certainly at the concentrations studied here, SAP mimics the effects of NPTX1 and also the effects of amyloidβ, as seen in the earliest stages of transgenic mice carrying familial Alzheimer's disease mutations (Cummings et al. 2015). Overall, the evidence presented here strongly suggests that SAP can enter the brain under some conditions and so would have the opportunity to interact with the NPTXs, influencing central synaptic transmission in Alzheimer's disease but also under other conditions of blood–brain barrier breakdown.

Supplementary Material

Supplementary material are available at *Cerebral Cortex* online.

Funding

Primary funding: MRC grant MR/J011851/1 to F.A.E. Alzheimer's Research UK Senior Fellowships to D.A.S. and T.L.; Faculty of Life Sciences, UCL: PhD studentship to T.A.B., partial funding to D.M.C.; Alzheimer's Research UK PhD studentship to C.E.M.

References

Abad MA, Enguita M, DeGregorio-Rocasolano N, Ferrer I, Trullas R. 2006. Neuronal pentraxin 1 contributes to the neuronal damage evoked by amyloid-beta and is overexpressed in dystrophic neurites in Alzheimer's brain. J Neurosci. 26: 12735–12747.

Abramov E, Dolev I, Fogel H, Ciccotosto GD, Ruff E, Slutsky I. 2009. Amyloid-beta as a positive endogenous regulator of release probability at hippocampal synapses. Nat Neurosci. 12:1567–1578.

Baltz ML, Gomer K, Davies AJ, Evans DJ, Klaus GG, Pepys MB. 1980. Differences in the acute phase responses of serum amyloid P-component (SAP) and C3 to injections of casein or bovine serum albumin in amyloid-susceptible and -resistant mouse strains. Clin Exp Immunol. 39:355–360.

Bien-Ly N, Boswell CA, Jeet S, Beach TG, Hoyte K, Luk W, Shihadeh V, Ulufatu S, Foreman O, Lu Y, et al. 2015. Lack of widespread BBB disruption in Alzheimer's disease models: focus on therapeutic antibodies. Neuron. 88: 289–297.

Blennow K, Wallin A, Fredman P, Karlsson I, Gottfries CG, Svennerholm L. 1990. Blood-brain barrier disturbance in patients with Alzheimer's disease is related to vascular factors. Acta Neurol Scand. 81:323–326.

Bottomley KM, Rising TJ, Steward A. 1988. The serum amyloid P response in the mouse air pouch. J Pharm Pharmacol. 40: 227–228.

Chang MC, Park JM, Pelkey KA, Grabenstatter HL, Xu D, Linden DJ, Sutula TP, McBain CJ, Worley PF. 2010. Narp regulates homeostatic scaling of excitatory synapses on parvalbumin-expressing interneurons. Nat Neurosci. 13:1090–1097.

Chen B, Bixby JL. 2005. Neuronal pentraxin with chromo domain (NPCD) is a novel class of protein expressed in multiple neuronal domains. J Comp Neurol. 481:391–402.

Chisholm KI, Ida KK, Davies AL, Tachtsidis I, Papkovsky DB, Dyson A, Singer M, Duchen MR, Smith KJ. 2015. Hypothermia protects brain mitochondrial function from hypoxemia in a murine model of sepsis. J Cereb Blood Flow Metab. 26: 1955–1964.

Cho RW, Park JM, Wolff SB, Xu D, Hopf C, Kim JA, Reddy RC, Petralia RS, Perin MS, Linden DJ, et al. 2008. mGluR1/5-dependent long-term depression requires the regulated ectodomain cleavage of neuronal pentraxin NPR by TACE. Neuron. 57:858–871.

Clayton KB, Podlesniy P, Figueiro-Silva J, Lopez-Domenech G, Benitez L, Enguita M, Abad MA, Soriano E, Trullas R. 2012. NP1 regulates neuronal activity-dependent accumulation of BAX in mitochondria and mitochondrial dynamics. J Neurosci. 32:1453–1466.

Cummings DM, Liu W, Portelius E, Bayram S, Yasvoina M, Ho SH, Smits H, Ali SS, Steinberg R, Pegasiou CM, et al. 2015. First effects of rising amyloid-beta in transgenic mouse brain: synaptic transmission and gene expression. Brain. 138:1992–2004.

De Simoni A, Griesinger CB, Edwards FA. 2003. Development of rat CA1 neurones in acute versus organotypic slices: role of experience in synaptic morphology and activity. J Physiol. 550:135–147.

De Simoni A, Yu LM. 2006. Preparation of organotypic hippocampal slice cultures: interface method. Nat Protoc. 1: 1439–1445.

Dobrunz LE, Stevens CF. 1997. Heterogeneity of release probability, facilitation, and depletion at central synapses. Neuron. 18:995–1008.

Duong T, Acton PJ, Johnson RA. 1998. The in vitro neuronal toxicity of pentraxins associated with Alzheimer's disease brain lesions. Brain Res. 813:303–312.

Edwards FA, Konnerth A, Sakmann B, Takahashi T. 1989. A thin slice preparation for patch clamp recordings from neurones of the mammalian central nervous system. Pflugers Arch. 414:600–612.

Figueiro-Silva J, Gruart A, Clayton KB, Podlesniy P, Abad MA, Gasull X, Delgado-Garcia JM, Trullas R. 2015. Neuronal pentraxin 1 negatively regulates excitatory synapse density and synaptic plasticity. J Neurosci. 35:5504–5521.

Hawkins PN. 1994. Studies with radiolabelled serum amyloid P component provide evidence for turnover and regression of amyloid deposits in vivo. Clin Sci (Lond). 87:289–295.

Hawkins PN, Rossor MN, Gallimore JR, Miller B, Moore EG, Pepys MB. 1994. Concentration of serum amyloid P component in the CSF as a possible marker of cerebral amyloid deposits in Alzheimer's disease. Biochem Biophys Res Commun. 201: 722–726.

Hawrylycz MJ, Lein ES, Guillozet-Bongaarts AL, Shen EH, Ng L, Miller JA, van de Lagemaat LN, Smith KA, Ebbert A, Riley ZL, et al. 2012. An anatomically comprehensive atlas of the adult human brain transcriptome. Nature. 489:391–399.

Iwanaga T, Wakasugi S, Inomoto T, Uehira M, Ohnishi S, Nishiguchi S, Araki K, Uno M, Miyazaki J, Maeda S. 1989. Liver-specific and high-level expression of human serum amyloid P component gene in transgenic mice. Dev Genet. 10:365–371.

Kalaria RN, Golde TE, Cohen ML, Younkin SG. 1991. Serum amyloid P in Alzheimer's disease. Implications for dysfunction of the blood-brain barrier. Ann N Y Acad Sci. 640: 145–148.

Kimura M, Asada T, Uno M, Machida N, Kasuya K, Taniguchi Y, Fujita T, Nishiyama E, Iwamoto N, Arai H. 1999. Assessment of cerebrospinal fluid levels of serum amyloid P component in patients with Alzheimer's disease. Neurosci Lett. 273:137–139.

Kirkpatrick LL, Matzuk MM, Dodds DC, Perin MS. 2000. Biochemical interactions of the neuronal pentraxins. Neuronal pentraxin (NP) receptor binds to taipoxin and taipoxin-associated calcium-binding protein 49 via NP1 and NP2. J Biol Chem. 275: 17786–17792.

Kolstoe SE, Ridha BH, Bellotti V, Wang N, Robinson CV, Crutch SJ, Keir G, Kukkastenvehmas R, Gallimore JR, Hutchinson WL, et al. 2009. Molecular dissection of Alzheimer's disease neuropathology by depletion of serum amyloid P component. Proc Natl Acad Sci USA. 106:7619–7623.

Lashley T, Rohrer JD, Bandopadhyay R, Fry C, Ahmed Z, Isaacs AM, Brelstaff JH, Borroni B, Warren JD, Troakes C, et al. 2011. A comparative clinical, pathological, biochemical and genetic study of fused in sarcoma proteinopathies. Brain. 134: 2548–2564.

Manepalli J, Grossberg GT, Mueller C. 1990. Prevalence of delirium and urinary tract infection in a psychogeriatric unit. J Geriatr Psychiatry Neurol. 3:198–202.

Matarin M, Salih DA, Yasvoina M, Cummings DM, Guelfi S, Liu W, Nahaboo Solim MA, Moens TG, Paublete RM, Ali SS, et al. 2015. A genome-wide gene-expression analysis and database in transgenic mice during development of amyloid or tau pathology. Cell Rep. 10:633–644.

Montagne A, Barnes SR, Sweeney MD, Halliday MR, Sagare AP, Zhao Z, Toga AW, Jacobs RE, Liu CY, Amezcua L, et al. 2015. Blood-brain barrier breakdown in the aging human hippocampus. Neuron. 85:296–302.

Mulder SD, Hack CE, van der Flier WM, Scheltens P, Blankenstein MA, Veerhuis R. 2010. Evaluation of intrathecal serum amyloid P (SAP) and C-reactive protein (CRP) synthesis in Alzheimer's disease with the use of index values. J Alzheimers Dis. 22:1073–1079.

Nelson SR, Tennent GA, Sethi D, Gower PE, Ballardie FW, Amatayakul-Chantler S, Pepys MB. 1991. Serum amyloid P component in chronic renal failure and dialysis. Clin Chim Acta. 200:191–199.

O'Brien RJ, Xu D, Petralia RS, Steward O, Huganir RL, Worley P. 1999. Synaptic clustering of AMPA receptors by the extracellular immediate-early gene product Narp. Neuron. 23:309–323.

Pelkey KA, Barksdale E, Craig MT, Yuan X, Sukumaran M, Vargish GA, Mitchell RM, Wyeth MS, Petralia RS, Chittajallu R, et al. 2015. Pentraxins coordinate excitatory synapse maturation and circuit integration of parvalbumin interneurons. Neuron. 85:1257–1272.

Pepys MB, Dash AC, Markham RE, Thomas HC, Williams BD, Petrie A. 1978. Comparative clinical study of protein SAP (amyloid P component) and C-reactive protein in serum. Clin Exp Immunol. 32:119–124.

Pepys MB, Hirschfield GM. 2003. C-reactive protein: a critical update. J Clin Invest. 111:1805–1812.

Pilling D, Gomer RH. 2012. Differentiation of circulating monocytes into fibroblast-like cells. Methods Mol Biol. 904: 191–206.

Pribiag H, Stellwagen D. 2014. Neuroimmune regulation of homeostatic synaptic plasticity. Neuropharmacology. 78:13–22.

Schlimgen AK, Helms JA, Vogel H, Perin MS. 1995. Neuronal pentraxin, a secreted protein with homology to acute phase proteins of the immune system. Neuron. 14:519–526.

Scotti AL, Chatton JY, Reuter H. 1999. Roles of Na+-Ca2+ exchange and of mitochondria in the regulation of presynaptic Ca2+ and spontaneous glutamate release. Philos T Roy Soc B. 354:357–364.

Sia GM, Beique JC, Rumbaugh G, Cho R, Worley PF, Huganir RL. 2007. Interaction of the N-terminal domain of the AMPA receptor GluR4 subunit with the neuronal pentraxin NP1 mediates GluR4 synaptic recruitment. Neuron. 55:87–102.

Stoppini L, Buchs PA, Muller D. 1991. A simple method for organotypic cultures of nervous tissue. J Neurosci Methods. 37: 173–182.

Tsui CC, Copeland NG, Gilbert DJ, Jenkins NA, Barnes C, Worley PF. 1996. Narp, a novel member of the pentraxin family, promotes neurite outgrowth and is dynamically regulated by neuronal activity. J Neurosci. 16:2463–2478.

Urbanyi Z, Lakics V, Erdo SL. 1994. Serum amyloid P component-induced cell death in primary cultures of rat cerebral cortex. Eur J Pharmacol. 270:375–378.

Urbanyi Z, Sass M, Laszy J, Takacs V, Gyertyan I, Pazmany T. 2007. Serum amyloid P component induces TUNEL-positive nuclei in rat brain after intrahippocampal administration. Brain Res. 1145:221–226.

Veszelka S, Laszy J, Pazmany T, Nemeth L, Obal I, Fabian L, Szabo G, Abraham CS, Deli MA, Urbanyi Z. 2013. Efflux transport of serum amyloid P component at the blood-brain barrier. Eur J Microbiol Immunol (Bp). 3:281–289.

Xu D, Hopf C, Reddy R, Cho RW, Guo L, Lanahan A, Petralia RS, Wenthold RJ, O'Brien RJ, Worley P. 2003. Narp and NP1 form heterocomplexes that function in developmental and activity-dependent synaptic plasticity. Neuron. 39:513–528.

Yasojima K, Schwab C, McGeer EG, McGeer PL. 2000. Human neurons generate C-reactive protein and amyloid P: upregulation in Alzheimer's disease. Brain Res. 887:80–89.

Zucker RS. 1989. Short-term synaptic plasticity. Annu Rev Neurosci. 12:13–31.